Mechanics of cell spreading: role of myosin II

Tetsuro Wakatsuki[1], Robert B. Wysolmerski[2] and Elliot L. Elson[1,*]

[1]Department of Biochemistry and Molecular Biophysics, Washington University School of Medicine, St Louis, MO 63110, USA
[2]Department of Pathology and Anesthesiology, St Louis University School of Medicine, St Louis, MO 63104, USA
*Author for correspondence (e-mail: elson@biochem.wustl.edu)

Accepted 2 January 2003
Journal of Cell Science 116, 1617-1625 © 2003 The Company of Biologists Ltd
doi:10.1242/jcs.00340

Summary

As it migrates over a substratum, a cell must exert different kinds of forces that act at various cellular locations and at specific times. These forces must therefore be coordinately regulated. The Rho-family GTPases Rac1 and Cdc42 promote actin polymerization that drives extension of the leading cell edge. Subsequently, RhoA regulates myosin-dependent contractile force, which is required for formation of adhesive contacts and stress fibers. During cell spreading, however, the activity of RhoA is reduced by a mechanism involving the tyrosine kinases c-Src and focal adhesion kinase (FAK), and the p190RhoGAP. It has been proposed that this reduction of RhoA activity facilitates edge extension by reducing myosin-dependent contractile forces that could resist this process. We have directly tested this hypothesis by correlating myosin activity with the rate of cell spreading on a substratum. The rate of spreading is inversely related to the myosin activity. Furthermore, spreading is inhibited by low concentrations of cytochalasin D, as expected for a process that depends on the growth of uncapped actin filaments. Cell indentation measurements show that a myosin-dependent viscoelastic force resists cell deformation.

Key words: Myosin II, Cell spreading, Cell mechanics, Traction force, Contraction, Cytochalasin D

Introduction

The dynamic behavior of cells often depends on a balance between forces that contract the cell into a more compact shape and forces that extend the boundaries of the cell and cause it to assume a less compact shape. Both kinds of forces are important both for cell locomotion and the remodeling of extracellular matrix (ECM) that occurs in tissue development and wound healing. Contractile forces can shift the center of gravity of a cell, detach it from a substratum, or compress and remodel the matrix in which it is embedded. Protrusive forces that cause cell spreading or extend lamellipodia and filopodia are also important for cell locomotion and to maximize the contact of cells with the matrix or substratum to which they adhere. Therefore, regulation of protrusive and contractile forces to achieve a balance appropriate for specific functions is essential for normal cell physiological behavior.

Much has recently been learned about the regulation of these forces. For example, when fibroblasts, initially spherical in suspension, encounter a substratum, they spread to a more flattened shape. This process is analogous to the forward extension of lamelllipodia and filopodia by polarized cells as they migrate over a substratum. This cell spreading is driven by actin polymerization that is promoted by the Rho-family GTPases Cdc42 and Rac1. These two molecules initiate polymerization by different pathways (Worthylake and Burridge, 2001). The former activates the Arp2/3 complex, which nucleates new actin filaments to form a dendritic actin filament network (Borisy and Svitkina, 2000). The latter uncaps the barbed ends of pre-existing filaments to permit them to grow further (Hartwig et al., 1995). After spreading, the cells form specialized structures such as stress fibers and focal adhesions that mediate adherence to the substratum. These processes require myosin-dependent contractile force that is activated by the RhoA GTPase- and calcium/calmodulin (CaM)-dependent pathways, which promote the phosphorylation of the regulatory light chain (RLC) of myosin II in nonmuscle cells (Amano et al., 1996; Kimura et al., 1996). The processes that regulate extension and adhesion are coordinated. During the initial cell spreading phase, binding of integrins to ECM ligands diminishes RhoA activity by activating p190RhoGAP via c-Src and FAK (Arthur and Burridge, 2001; Ren et al., 1999; Ren et al., 2000). This observation suggests the hypothesis that RhoA is deactivated to diminish the myosin contractile force that would otherwise impede cell spreading. This hypothesis predicts that the rate of cell spreading should vary inversely with myosin activity. In this work, we have tested this hypothesis by correlating the activity of myosin, measured in terms of the extent of phosphorylation of its RLC, with the rate of spreading of chicken embryo fibroblasts (CEFs).

As indicated above, current models suppose that the extension of the cell is propelled by the growth of actin filaments that incorporate actin monomers at their barbed ends. This hypothesis predicts that the barbed ends of the participating filaments are free (i.e. are not blocked by barbed-end capping proteins). If this is true, the filaments should bind cytochalasin D (CD) at close to nanomolar concentrations in the range of the binding constant measured for free actin filaments (Cooper, 1987). Therefore, edge extension should be inhibited by CD at sub-nanomolar concentrations in contrast to the effects of CD on cell shape and deformability that require much higher (μM) concentrations to compete with barbed-end

capping proteins bound to actin filaments (Wakatsuki et al., 2001). We have tested this hypothesis by determining the concentrations at which CD inhibits cell spreading.

A further hypothesis is that activation of myosin promotes interaction of myosin with actin filaments anchored to the plasma membrane, thereby increasing cell stiffness and consequently resistance to cell extension driven by actin polymerization. This hypothesis predicts that the stiffness of the cell should be increased by myosin activation. Using a cell indentation assay to measure cell stiffness, we have tested and confirmed this hypothesis.

Materials and Methods

Quantitative cell spreading assay

Prior to the experiments, the CEFs were incubated with DMEM containing 3% FBS. They were detached from the substratum by a brief exposure (<5 minutes) to 0.25% trypsin in EDTA containing glucose-supplemented PBS. Soybean trypsin inhibitor was added to the solution to quench the trypsin activity. The suspended CEFs were collected, centrifuged and resuspended in serum-free DMEM after discarding the supernatant. The cell concentration was adjusted to 100,000 cells/ml for re-plating in 35 mm tissue culture dishes for the spreading assay. Serum-free DMEM, mixed with a compound to be tested or with the solvent in which the compound was dissolved, was poured into each culture dish prior to addition of the suspended cells in serum-free DMEM. Therefore, a dish of cells was prepared for each of the time points in the measurement and an equal number of dishes of cells was also prepared for measurements of myosin RLC phosphorylation. Cell spreading was started by pouring the cell suspension in serum-free DMEM into the dishes prepared as described above. At each time point, the cell spreading was stopped by pouring off the medium and incubating with 3.7% formaldehyde in PBS for 20 minutes at room temperature. The cells were permeabilized in 0.2% Triton X-100 and incubated with 10% crystal violet solution in ethanol to stain cytoplasm to enhance contrast for microscopy. At least three images from different regions of the dish were captured by video camera through a Zeiss IM-35 inverted microscope (Thornwood, NY) in bright field mode. The digitized images were stored in a personal computer through a frame-grabber (Scion Corporation, Frederick, MD). The edges of individual cells were traced by hand and the area enclosed by the trace was measured using Scion Image software (Scion Corporation). The statistical analysis of the data was carried out using Origin software (Microal Software, Northampton, MA). Each data point represents an average of at least 30 individual measurements of the area.

The degree of cell spreading was also measured with different concentrations of CD (Sigma) in the presence of staurosporine (STA) or KT5926 (KT). Each 35 mm dish contained the same concentration of STA (100 nM) or KT (1 μM) and cells (100,000/dish) but a different concentration of CD. The cell spreading was stopped and measured 1 hour after the seeding of cells in each dish as described above. The CD and STA, or CD and KT, were present in the medium throughout the experiment. The half-maximum concentration of CD to inhibit cell spreading was determined by fitting a sigmoidal curve to the data shown in Fig. 3. Stock solution (2 mM) of CD was made in DMSO.

Myosin RLC phosphorylation

At each time point during cell spreading, after discarding the culture medium, the dishes were incubated with a solution containing 1 ml 10% TCA and 10 mM dithiothreitol (DTT). The precipitate was scraped from the dishes and washed three times each with 1 ml of acetone containing 10 mM DTT. After centrifugation, the pellets were solubilized in loading buffer containing 9 M urea, 2 mM DTT, 20 mM Tris, 22 mM glycine and 250 mM sucrose. The phosphorylated myosin RLCs were separated in 1 mm thick mini-gels containing 40% glycerol, 10% acrylamide, 20 mM Tris and 22 mM glycine. The detailed experimental procedures are presented elsewhere (Goeckeler et al., 2000). Polyclonal rabbit antibody to recombinant myosin II RLC was used to detect the light chains (Chew et al., 1998).

Compounds inhibiting myosin II activities

To inhibit myosin activity, samples were treated with 100 nM STA (Sigma) or 1 μM KT (Calbiochem, La Jolla, CA) dissolved in DMSO (<0.1% of the total volume of the medium). The cells were not pretreated with any other compounds. A small amount of medium containing resuspended cells was pipetted into the medium already mixed with STA or KT at its final concentration. Control samples contained the same amount of DMSO as the samples treated with STA and KT.

Confocal immunofluorescence microscopy

F-actin was stained with rhodamine-labeled phalloidin. Myosin II was immunolocalized using antibodies specific for myosin II (Goeckeler and Wysolmerski, 1995) and an Alexa-labeled secondary antibody. The fluorescent images of actin filaments and myosin II were taken using scanning confocal microscopy (Bio-Rad, Hercules, CA).

Indentation stiffness measurements of single cells

The indenter consists of a vertical glass stylus with a tip about 2 μm in diameter connected to a linear piezoelectric motor by a glass beam of known bending constant. The vertical position of the stylus tip is monitored optically by measuring the light reflected from a flag attached to the tip. The force exerted on the tip by the resistance of the cell to indentation is calculated by measuring the bending of the beam (Zahalak et al., 1990). The point at which bending of the beam is first detected indicates the initial contact of the tip with an object. This position indicates the height of the object relative to the substratum. A reference position was established for each cell by probing the substratum near the cell.

Results

Myosin RLC phosphorylation during cell spreading without serum

The CEFs can spread on tissue culture plates without serum. After 24 hours of cell culture, fluorescence microscopy shows actin filaments labeled with rhodamine-phalloidin in stress fibers and vinculin labeled with immunostaining forming focal adhesions (results not shown). The extent of phosphorylation of myosin RLCs in the suspended cells was surprisingly high (~50%) (result not shown), and it diminished after adhesion of the cells to a rigid substratum. Then, during cell spreading, 30-40% of the myosin RLC remained phosphorylated and eventually increased again up to ~50% after 2 hours even without serum (Fig. 1). Tryptic peptide mapping (Goeckeler and Wysolmerski, 1995) confirmed that the sites of phosphorylation were Ser19 and Thr18 of myosin RLC, which are the residues responsible for myosin activation (results not shown). This level of myosin RLC seems to be phosphorylated even without added mitogenic factors. The binding of the cell to the rigid substratum might maintain this amount of myosin RLC phosphorylation at later times, although the initial cell adhesion causes a decrease in myosin RLC phosphorylation.

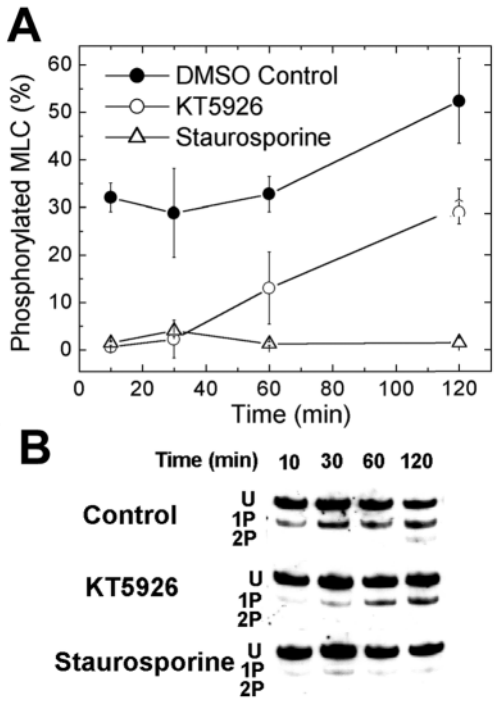

Fig. 1. Myosin activity during cell spreading with and without STA and KT. During cell spreading, 30-40% of the myosin RLC was phosphorylated at a steady level for 1 hour and the RLC was further phosphorylated at 2 hours after spreading even without serum (●). The specific RLC kinase inhibitor KT (1 μM) reduced the amount of the phosphorylated RLC to less than 10% of the total RLC for 30 minutes after re-plating (○). The relatively nonspecific kinase inhibitor STA (100 nM) (△) suppressed the RLC phosphorylation to less than 5% for a much longer period (2 hours) compared with KT. The quantitative level of RLC phosphorylation (A) was detected by modified western blots (B). Data represent the averaged value of at least three independent experiments (A). U, 1P and 2P indicate unphosphorylated, mono-phosphorylated and di-phosphorylated myosin light chains respectively (B).

KT and STA accelerate cell spreading

Can cells spread in the absence of myosin II activity? We used kinase inhibitors to prevent activation of myosin by phosphorylation of the myosin RLC, and the effects of the inhibitors on the levels of myosin RLC phosphorylation were measured. A specific myosin RLC kinase inhibitor KT (1 μM) reduced the amount of the phosphorylated RLC to almost an undetectable level at 10 minutes after re-plating. Then the level of phosphorylation began to climb, reaching almost 30% by 2 hours (Fig. 1). The relatively nonspecific kinase inhibitor STA (100 nM) suppressed the myosin RLC phosphorylation to less than 5% for the entire 2-hour measuring period (Fig. 1).

The inhibitors of myosin RLC phosphorylation, KT and STA, accelerated cell spreading. Although the total projected area at the end of 2 hours was almost indistinguishable for cells in the presence and absence of KT and STA, the difference in spreading area at 30 minutes and 60 minutes between treated and nontreated groups was statistically significant ($P<0.05$) (Fig. 2). We conclude that myosin II contributes little to the protrusion of the leading edge of a spreading cell. Indeed, cell spreading could occur with an almost undetectable level of myosin II activity. The cell spreading apparently is retarded by the myosin II activity. These observations raise a simple question: what is the major force driving protrusion of cell edges during cell spreading? The most reasonable candidate is actin polymerization. If we could test a specific inhibitor of actin polymerization in combination with the myosin inhibitor, the contribution of actin polymerization to cell spreading would be clarified.

Low dose of CD inhibits cell spreading

We used CD to test the importance of actin polymerization in cell spreading while myosin II activity was suppressed. Although the mechanisms by which CD affects the organization of the actin cytoskeleton are complex in detail (Cooper, 1987), at the low concentrations used in these experiments the main effect of CD arises from its binding to the barbed end of actin filaments, thereby both inhibiting actin polymerization and competing with capping proteins for binding to the barbed ends (Wakatsuki et al., 2001). The dependence of the projected cell area on the concentration of CD was observed for cells treated with STA and KT. The area measurements were well fitted to sigmoidal curves plotted on semi-logarithmic scale to yield an effective half-maximum inhibitory dose (IC_{50}) of CD pretreated with STA and KT of approximately 3.5 nM and 20 nM, respectively (Fig. 3). These are much closer to the estimated dissociation constant (2 nM) for the binding of CD to the barbed end of actin filaments in vitro (Cooper, 1987) than those estimated or used for F-actin disruption (Wakatsuki et al., 2001). Despite the complexity of the action of CD in vivo (Cooper, 1987), the close match to Kd suggests that the inhibitory effect of CD resulted from its binding to the barbed ends of actin filaments with little competition from capping proteins. This further suggests that actin filaments undergoing polymerization during the protrusion of the leading edge are essentially free at their barbed ends. Since myosin II-dependent actin reorganization was suppressed by STA or KT, these results support the hypothesis that the protrusion of the leading cell edge requires actin polymerization but not myosin II. Nevertheless, the possible involvement of other motor proteins not inhibited by STA or KT cannot be ruled out.

Actin and myosin II localization during cell spreading with and without STA and KT

Active myosin II binds actin filaments and bundles them to form stress fibers. Myosin II visualized by immunostaining co-localized with actin filaments labeled with rhodamine-phalloidin. Together, they began to resemble stress fibers 60 minutes after the initiation of cell spreading without KT and STA (result not shown). Under the same conditions at 120 minutes, stress fibers were indicated clearly by a strong co-localization of myosin II with actin filaments (Fig. 4M). Suppressing myosin II activity by KT and STA abolished the co-localization of myosin II with actin filaments. The KT and STA treatments increased the number of filopodia and induced extension of lamellipodia earlier than in the control cells (Fig. 4A-C). Thus, cells treated with KT and STA spread much faster than cells without them (Fig. 4G-I). The increased rate of cell spreading in the presence of KT and STA also caused the cells

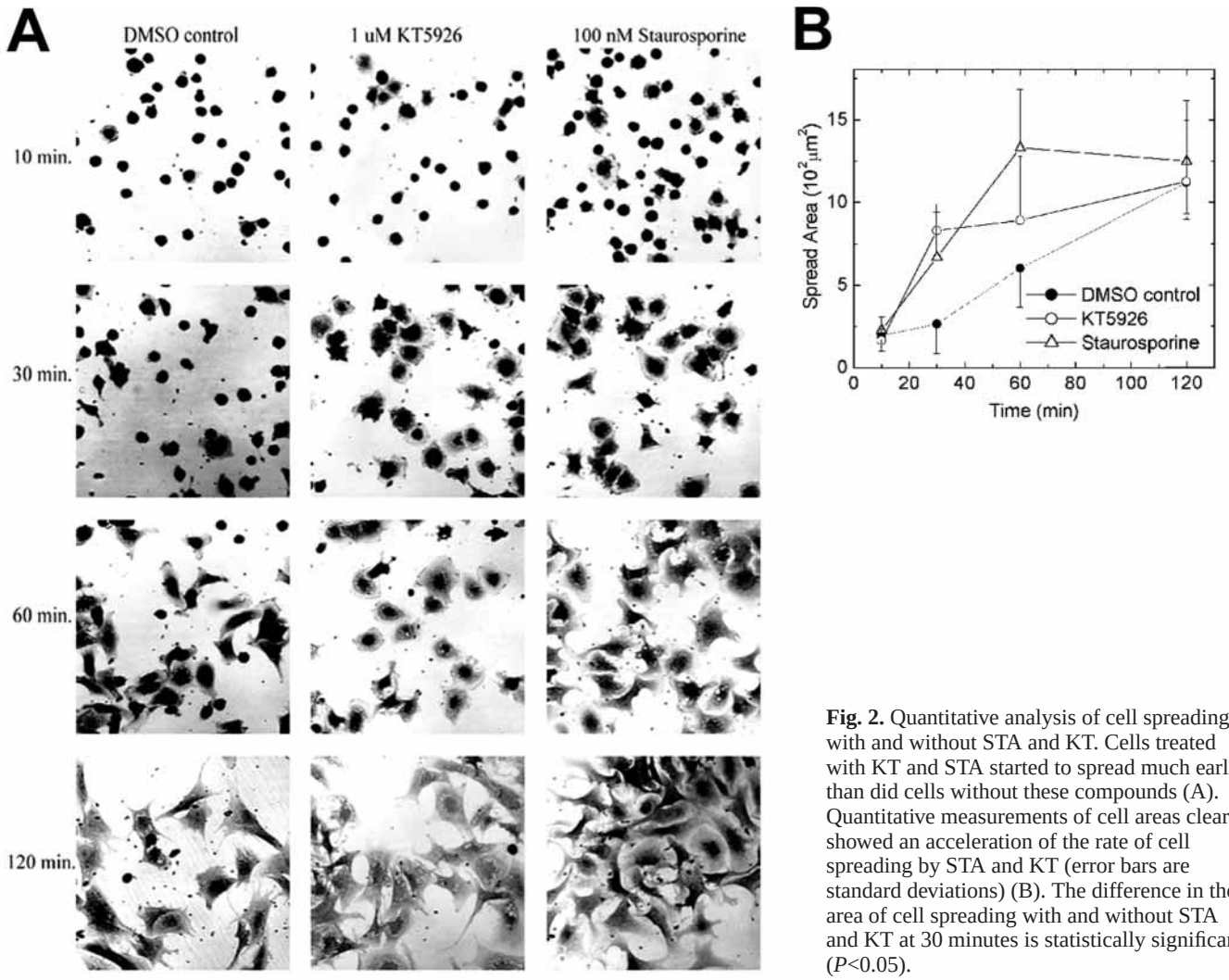

Fig. 2. Quantitative analysis of cell spreading with and without STA and KT. Cells treated with KT and STA started to spread much earlier than did cells without these compounds (A). Quantitative measurements of cell areas clearly showed an acceleration of the rate of cell spreading by STA and KT (error bars are standard deviations) (B). The difference in the area of cell spreading with and without STA and KT at 30 minutes is statistically significant (P<0.05).

to flatten earlier. This was visualized in cross-sectional images of cells taken by confocal microscopy (Fig. 4D-F,J-L). In some cells treated with straurosporine for 60 minutes, the actin filaments began to assume a dispersed distribution and, by 120 minutes, many of the cells began to break apart (Fig. 4O). A similar breakage of keratocytes by STA treatment has been reported (Verkhovsky et al., 1999b). The cells treated with KT-5926 never show this kind of fragmentation. Instead, at 120 minutes, a co-localization of myosin II and actin filaments (Fig. 4N), which correlated with the increase in myosin II activity, began to appear in KT5926-treated cells as shown in Fig. 1. The localization of myosin II and actin with and without STA and KT was consistent with the activity of myosin II shown in Fig. 1 and the rate of cell spreading shown in Fig. 2. However, at 10 minutes of cell spreading, myosin II was localized diffusely in the entire cytoplasm with or without STA and KT, despite the difference in myosin RLC phosphorylation noted above. The association of active myosin II with F-actin might be difficult to visualize by fluorescence microscopy in the early stages of cell spreading.

Cell deformability

In the early stages of cell spreading, the extent of actin filament crosslinking by active myosin could be less than at later stages, when stress fibers are formed (Fig. 4M). The crosslinking of actin filaments by α-actinin increases viscoelasticity of actin networks (Sato et al., 1987). If active myosin II crosslinks actin filaments, the viscoelastic properties of cells treated with KT should be different from those of untreated cells. We have suggested that activation of myosin retards spreading of a cell by increasing its resistance to deformation (i.e. its stiffness). To test this hypothesis, we measured cell stiffness by an indentation method in the early stages of spreading (initial 10-30 minutes). These measurements are similar in concept to atomic force microscopy. The tip of a probe mounted on a cantilever with known Young's Modulus indents the cell. The bending of the cantilever is translated into the force required for indentation (Zahalak et al., 1990). This approach yields the heights of cells by comparing the positions at which the cantilever begins to bend due to initial contacts of the probe with the cell and with the substratum. In this way, we have confirmed that KT caused the cells to become flatter than control cells (Fig. 5A), as was observed in cross-sectional confocal microscopic images (Fig. 4D,E,J,K).

KT reduced cellular stiffness. The forces required to indent single cells with or without treatment by KT are plotted against % indentation (Fig. 5B). In these measurements, the tip is

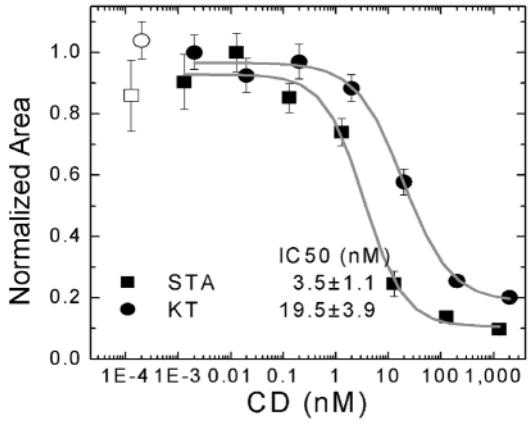

Fig. 3. Effect of CD concentration on STA- and KT-treated cells. The dependence of cell area on CD concentration was observed for STA or KT-treated cells spreading for 30 minutes (error bars are standard errors of at least 20 measurements). The sigmoidal curve was well fit to the data plotted on the semi-logarithmic scale and yielded the effective half-maximum inhibitory dose (IC_{50}) of CD on STA- and KT-pretreated cells of 3.5 nM and 20 nM, respectively.

lowered at a constant rate to indent the cell ('loading') and is then retracted at the same rate ('unloading'). KT reduced both the resistance force and the slope (stiffness) of the loading curve (Fig. 5B).

Discussion

Spreading rate varies inversely with myosin activity

Cellular dynamic functions such as locomotion, wound healing and tissue remodeling require that cells regulate and balance the different types of forces that they exert on themselves and their surroundings. When cells first reach a substrate, they spread to maximize surface contact. When they migrate, they extend forward lamellipodia and filopodia to form advanced surface contacts. These processes require forces that extend cells from more- to less-compact shapes. Conversely, once cells have spread, they form structures including stress fibers and focal adhesions that anchor them to the substrate or matrix. These latter processes require cellular contractile force. Therefore, when performing different physiological processes, cells must exert opposing extensile or contractile forces. The balance of these forces must be actively regulated by a cell in order to drive the specific dynamic functions in which it engages (T.W. and E.L.E., unpublished).

Both extending and contracting forces are regulated by Rho-family GTPases. Much recent evidence indicates that actin polymerization drives cell spreading and forward extension during migration (Borisy and Svitkina, 2000; Pollard et al., 2000). Two Rho-family GTPases, Rac1 and Cdc42, promote polymerization either by uncapping the barbed (rapidly polymerizing) ends of pre-existing actin filaments or by activating the Arp2/3 complex to nucleate new actin filaments at the sides of pre-existing filaments, thereby forming a dendritic network (Worthylake and Burridge, 2001). Another member of this family, RhoA, promotes formation of stress fibers and focal adhesions by elevating contractile force (Burridge and Chrzanowska-Wodnicka, 1996; Elbaum et al., 1999). Rho A activates nonmuscle myosin by increasing the level of phosphorylation of its RLC (Amano et al., 1996; Kimura et al., 1996).

Depending on their relative magnitudes, the balance of forces arising from actin polymerization and myosin-dependent contraction will favor either extension or contraction of the cell margins. Evidently, this balance must vary during cell locomotion, spreading and adherence on a substrate. Biphasic regulation of Rho has been demonstrated when Swiss 3T3 cells adhere to fibronectin-coated substrata (Ren et al., 1999). A transient inhibition of Rho activity when the cells first contact the substratum is followed by an increase in Rho activity. The initial inhibition of Rho requires the tyrosine kinase FAK (Ren et al., 2000). In neutrophils, the mechanism of inhibition appears to operate through the oncogene c-Src, which by tyrosine phosphorylation activates p190RhoGAP, an inhibitor of Rho activity (Arthur and Burridge, 2001). These observations suggest that early inhibition of Rho upon contact with integrins might correspondingly inhibit myosin-dependent contractile forces that would resist cell spreading or the extension of the leading edge of migrating cells (Arthur and Burridge, 2001). For this hypothesis to be correct, the rate of cell spreading must vary inversely with myosin activity.

We have directly tested and confirmed this hypothesis by measuring the rate of spreading under conditions in which myosin activity is either inhibited, at a baseline level, or activated. In agreement with prediction, the rate of extension decreases as the level of myosin phosphorylation, and therefore myosin activity, increases (Figs 1, 2). In neutrophils, contact with peptides containing an RGD sequence, simulating interaction with an ECM ligand, had no effect on the activities of Cdc42 and Rac (Arthur et al., 2000). On the basis of early observations that edge extension continued even after contractile forces began to elevate a lamellipodium in the early stages of 'ruffle' formation (Felder and Elson, 1990), it appears that actin polymerization continues while myosin-dependent contractile forces increase.

We have observed that the level of myosin phosphorylation was surprisingly high (50%) in serum-starved cells and that this level at first decreased when the cells become adherent and then increased back to 50%. In earlier work, it was observed that while activation of Rho by lysophosphatidic acid was comparable in suspended and adherent cells, the Rho activity in adherent cells declined while that of suspended cells remained high (Ren et al., 1999). This suggests that there is an adherence-dependent system for regulating myosin activation through Rho (Arthur and Burridge, 2001; Ren et al., 1999).

Effects of inhibitors

Our results depend on using the kinase inhibitors KT and STA to reduce myosin activity. These inhibitors have different target specificities. KT is specific for the myosin light chain kinase (MLCK) (Nakanishi et al., 1990) and hence inhibits calcium-ion-dependent myosin activation. STA has a broad specificity for many protein kinases including MLCK, Rho kinase, protein kinase A (PKA), PKC and CaM kinase. However, as we have confirmed (Fig. 1), STA does inhibit myosin RLC phosphorylation very effectively (Sakurada et al., 1998).

Because of the higher specificity of KT, the relationship between its inhibition of myosin and the acceleration of

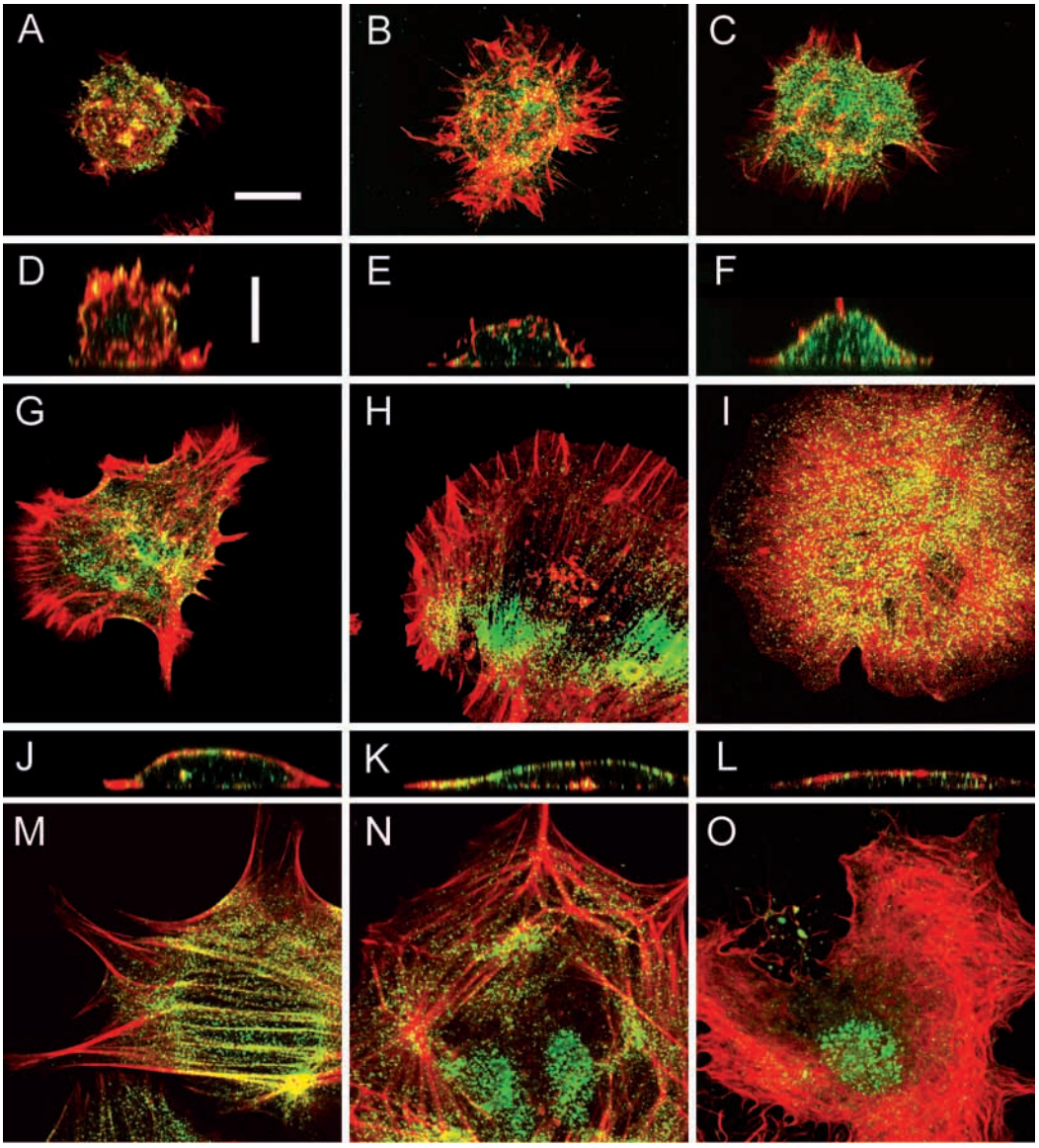

Fig. 4. Localization of actin and myosin II during cell spreading. Actin was stained with rhodamine-labeled phalloidin, and myosin II was immunolocalized using myosin II antibodies stained with Alexa-488-labeled secondary antibody. The cells shown in the images in the first (A,D,G,J,M), second (B,E,H,K,N) and third (C,F,I,L,O) column from the left are treated with DMSO, KT and STA, respectively. The cells shown in the first/second rows (A-F) and third/fourth rows (G-L) and the last row (M-O) of the images are fixed 10, 30 and 120 minutes after seeding the cells on the dishes, respectively. At 10 minutes after beginning cell spreading, myosin II was localized diffusely with or without STA and KT, yet the samples treated with STA and KT showed many F-actin spikes (A-C). Cross-sectional views of the cells in A-C are shown in D-F, whose cell heights were significantly reduced by myosin II inhibition. At 30 minutes, control cells started to spread asymmetrically, but cells treated with STA and KT were spread into almost circular shapes (G-I). This suggests that myosin might be required for polarization of spreading cells. Localization of myosin II at this stage was not different with or without the KT and STA. Cross-sectional views of cells showed significant differences in flattening of cells due to the increased rate of cell spreading in KT- and STA-treated cells (J-L). The myosin II strongly co-localized with actin filaments at 120 minutes without STA and KT (M). Cells treated with KT also started to show co-localization with actin filaments, which is consistent with the level of myosin RLC phosphorylation shown in Fig. 2 (N). Many cells treated with STA started to break into fragments (O).

spreading (Figs 1, 2) seems relatively straightforward. Nevertheless, we emphasize that the correlation of myosin inhibition with acceleration of spreading is seen with both inhibitors. STA inhibits myosin significantly longer than does KT. Although both STA and KT initially abolished myosin RLC phosphorylation almost completely, phosphorylation began to increase after 1 hour of spreading in the cells treated with KT, whereas STA continued to inhibit the RLC phosphorylation throughout the entire 2-hour observation period (Fig. 2). This was also confirmed visually by localization of myosin II and actin filaments (Fig. 4). Since STA has a broader specificity, this difference suggests the involvement of kinases other than MLCK after 60 minutes of cell spreading. The most attractive candidate is Rho kinase,

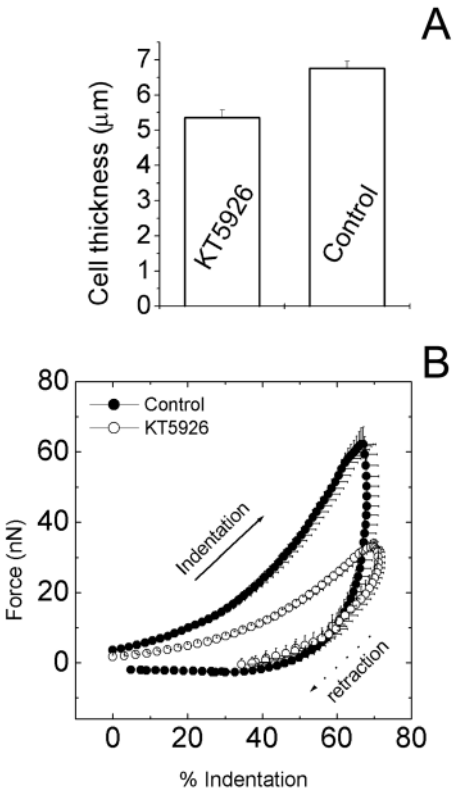

Fig. 5. Mechanical properties of cells with and without KT at early stages of cell spreading. The indentation measurements were performed on cells spreading 10-30 minutes after they settled on the substratum. The first point of contact on the cell made by a vertical cylindrical tip as well as the initial distance of the tip from the substratum were observed by indentation on the cell and the substrate next to the cell. The difference between them is the cell height shown in A. As we observed fixed cells by microscopy (Fig. 4), the heights of live cells treated with KT are significantly reduced (P<0.05) compared with those of control cells (A). Force responses to indentation by the cylindrical tip were plotted against % indentation (B). The data represent averaged values and standard errors of 25 and 15 cells with and without KT, respectively. The curve has an indentation phase (loading) indicated by a solid arrow and a retraction phase (unloading) indicated by a dotted arrow. The indentation phase force responses showed a significant reduction of stiffness in KT-treated cells compared with the control. The retraction phase for control cells showed no significant change in KT-treated cells (B).

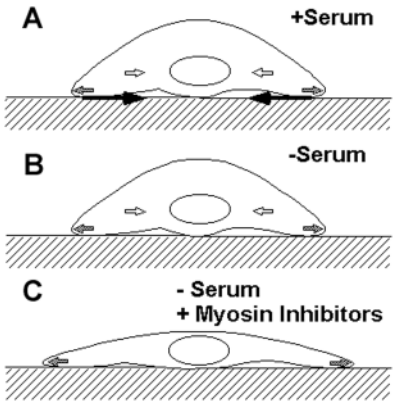

Fig. 6. Forces involved in cell spreading. Myosin II maintains the integrity of the actin cytoskeleton (small white arrows) as well as generating the traction force on the substratum (large black arrows). In the presence of serum, myosin II is fully activated. Hence the traction force is detectable (A). Without serum, the traction force is not detectable; either with or without serum, myosin II activity lasts briefly and counterbalances the protruding force (small gray arrows) due to actin polymerization (B). Hence, the traction force is not detectable. When myosin II activity is inhibited, the cell can spread without the counterbalancing force (C). Therefore, inhibition of myosin II activity increases the rate of cell spreading.

which is a target of STA (Feng et al., 1999). Inhibition of Rho kinase could interfere with RLC phosphorylation either directly or indirectly via the effect of Rho kinase on myosin phosphatase (Kureishi et al., 1997). The enhancement of endothelial cell spreading by the Rho kinase-specific inhibitor Y27632 has been observed recently (R.B.W. and G. M. Grojean, unpublished). Further investigation is required to clarify temporal differences in the regulation of cell spreading by MLCK and Rho kinase.

It has been reported that 2,3-butanedione monoxime (BDM) inhibits cell spreading (Sanders et al., 1999). Since BDM could inhibit ATPase activity of myosin isoforms other than myosin II, this observation could suggest involvement of different myosin isoforms in cell spreading. However, in our experiments, BDM (20 mM) treatment interfered with the adherence of CEFs to the tissue culture dishes (result not shown). This additional cellular response complicates the interpretation of the effect of BDM on contractility and myosin II function in cell spreading. BDM has been reported recently to have nonspecific and weak inhibitory effects on nonmuscle myosin (Cheung et al., 2001).

In addition to confirming the correlation between myosin inhibition and acceleration of spreading, the results obtained using STA are interesting because of the differences observed between its effects and those obtained with KT. These results clearly show that, although we cannot yet identify them, other STA targets are involved in myosin regulation and also in actin polymerization, as indicated below. More work is required to find the kinases responsible for these additional effects.

The actin filaments responsible for spreading are uncapped

To explain the effects of CD on cell shape and mechanical properties, it is necessary to take into account that most of the actin filaments in a cell are capped. Therefore, even though the binding of CD to the free barbed ends of actin filaments occurs with an affinity constant of ~2 nM (Cooper, 1987), it is necessary to use CD concentrations in the micromolar range to cause cells to round up and soften. This discrepancy is readily explained as a consequence of the competition between CD and endogenous capping proteins that bind the barbed ends of actin filaments (Wakatsuki et al., 2001). By contrast, the concentrations of CD effective for inhibition of cell spreading pretreated with STA and KT are 3.5 nM and 20 nM respectively. Therefore, the actin filaments that contribute to spreading are uncapped, as expected if they are growing by addition of new actin monomers to their barbed ends. That the concentrations of CD effective to inhibit spreading are lower in the presence of STA than with KT suggests that additional

STA targets beyond MLCK regulate uncapping activity during initial stages of cell spreading.

The retardation of cell spreading by active myosin correlates with increased cell stiffness

Our indentation measurements indicate that the retardation of cell spreading with increased myosin activity results from a myosin-dependent increase of cellular stiffness. The increased stiffness resists the protrusive force supplied by actin polymerization. Increased stiffness due to the action of nonmuscle myosin has been demonstrated in lymphocytes and *Dityostelium* amoebae (Pasternak and Elson, 1985; Pasternak et al., 1989). These studies were carried out by measuring cell stiffness as the resistance to indentation by a small probe (Petersen et al., 1982; Zahalak, 1986). We have used this same approach to measure cell deformation at rates comparable with the rates at which the cell changes shape. The specific inhibition of MLCK by KT reduces myosin activity and consequently leads to a reduction of contractile force and cellular stiffness (Fig. 5B). This supports our hypothesis that KT facilitates cell spreading by reducing cell stiffness.

A quantitative mechanical model of the cell is not yet available, and so we cannot provide a definitive structural interpretation of these observations. (Simple linear models such as the linear standard solid cannot explain this behavior.) Nevertheless, the measurements reported here are sufficient to confirm the predicted correlations between myosin activation and cell stiffness and their inverse correlation with rates of cell spreading. The active retrograde flow of myosin II observed in strongly adherent cells (Verkhovsky et al., 1999a) could be another factor that retards cell spreading. Membrane tension is also one of the physical factors that influence the rate of cell spreading by opposing actin polymerization (Raucher and Sheetz, 2000). Our measurements have demonstrated a shifting balance between a protrusive force due to actin polymerization and a myosin-dependent retarding force that also controls the rate of cell spreading.

Cell spreading and traction force

Cells exert a traction force on the substratum over which they migrate. The traction force was demonstrated on 2D surfaces by qualitatively observing the formation of wrinkles on ultra-thin silicon rubber films (Harris et al., 1981), and more quantitatively by several groups (Balaban et al., 2001; Dembo et al., 1996; Galbraith and Sheetz, 1997). The existence of the traction force was first demonstrated in 3D by Stopak and coworkers observing the contraction of cell-populated collagen matrices (CPM) (Bell et al., 1979; Grinnell, 1994; Stopak and Harris, 1982). We have directly measured these forces during CPM contraction by connecting the collagen matrix to an isometric force transducer. Contractile force increased significantly while cells are spreading into the collagen matrices in the presence of serum (Wakatsuki and Elson, 2003). However, we have found that, in a culture medium lacking serum, cells can spread into a matrix without causing substantial matrix remodeling and production of contractile force (Wakatsuki and Elson, 2003). A similar result was obtained by tracking the movement of small beads embedded around the fibroblasts in a collagen matrix (Roy et al., 1999). These observations suggest that a traction force is unnecessary for cell spreading or that the minimum traction force required for cell spreading could be too small to detect using the available methods.

Summary

We have analyzed the contribution of myosin II to cell spreading on 2D substrates. Our results are schematically summarized in Fig. 6. Reducing myosin II activity by inhibiting phosphorylation of myosin RLCs increased the rate of spreading. The protrusion of the lamella observed under myosin II inhibition was most likely due to actin polymerization (small dark arrow in Fig. 6), as was demonstrated by inhibiting cell spreading using low concentrations of CD under conditions of myosin inhibition. While cells with serum exert large traction forces during spreading, cells without serum hardly exert any traction forces. The low level of myosin II activity detected without serum could be required to maintain the integrity of the actin cytoskeleton (white arrow in Fig. 6). Consistent with observations on fish epidermal keratocytes (Verkhovsky et al., 1999b), we have shown that STA treatment of CEFs causes them to fragment. The results of cell indentation measurements suggest that inhibition of myosin activation by KT decreased cytoplasmic stiffness possibly by decreasing the crosslinking of actin filaments by myosin. This decrease of stiffness was then responsible for the observed increased cell deformability and the increased rate of cell spreading.

This work was supported in part by the National Institutes of Health Grants HL-45788 and GM-38838

References

Amano, M., Ito, M., Kimura, K., Fukata, Y., Chihara, K., Nakano, T., Matsuura, Y. and Kaibuchi, K. (1996). Phosphorylation and activation of myosin by Rho-associated kinase (Rho-kinase). *J. Biol. Chem.* **271**, 20246-20249.

Arthur, W. T. and Burridge, K. (2001). RhoA inactivation by p190RhoGAP regulates cell spreading and migration by promoting membrane protrusion and polarity. *Mol. Biol. Cell* **12**, 2711-2720.

Arthur, W. T., Petch, L. A. and Burridge, K. (2000). Integrin engagement suppresses RhoA activity via a c-Src-dependent mechanism. *Curr. Biol.* **10**, 719-722.

Balaban, N. Q., Schwarz, U. S., Riveline, D., Goichberg, P., Tzur, G., Sabanay, I., Mahalu, D., Safran, S., Bershadsky, A., Addadi, L. et al. (2001). Force and focal adhesion assembly: a close relationship studied using elastic micropatterned substrates. *Nat. Cell Biol.* **3**, 466-472.

Bell, E., Ivarsson, B. and Merrill, C. (1979). Production of a tissue-like structure by contraction of collagen lattices by human fibroblasts of different proliferative potential in vitro. *Proc. Natl. Acad. Sci. USA* **76**, 1274-1278.

Borisy, G. G. and Svitkina, T. M. (2000). Actin machinery: pushing the envelope. *Curr. Opin. Cell Biol.* **12**, 104-112.

Burridge, K. and Chrzanowska-Wodnicka, M. (1996). Focal adhesions, contractility, and signaling. *Annu. Rev. Cell Dev. Biol.* **12**, 463-518.

Cheung, A. J., Westwood, N. J., Chen, I., Mitchision, T. J. and Straight, A. F. (2001). Blebbistatin: a cell permeable ihibitor of non-muscle myosin II. *Mol. Biol. Cell* **12**, 271a.

Chew, T. L., Masaracchia, R. A., Goeckeler, Z. M. and Wysolmerski, R. B. (1998). Phosphorylation of non-muscle myosin II regulatory light chain by p21-activated kinase (gamma-PAK). *J. Muscle Res. Cell Motil.* **19**, 839-854.

Cooper, J. A. (1987). Effects of cytochalasin and phalloidin on actin. *J. Cell Biol.* **105**, 1473-1478.

Dembo, M., Oliver, T., Ishihara, A. and Jacobson, K. (1996). Imaging the

traction stresses exerted by locomoting cells with the elastic substratum method. *Biophys. J.* **70**, 2008-2022.

Elbaum, M., Chausovsky, A., Levy, E. T., Shtutman, M. and Bershadsky, A. D. (1999). Microtubule involvement in regulating cell contractility and adhesion-dependent signalling: a possible mechanism for polarization of cell motility. *Biochem. Soc. Symp.* **65**, 147-172.

Felder, S. and Elson, E. L. (1990). Mechanics of fibroblast locomotion: quantitative analysis of forces and motions at the leading lamellas of fibroblasts. *J. Cell Biol.* **111**, 2513-2526.

Feng, J., Ito, M., Kureishi, Y., Ichikawa, K., Amano, M., Isaka, N., Okawa, K., Iwamatsu, A., Kaibuchi, K., Hartshorne, D. J. et al. (1999). Rho-associated kinase of chicken gizzard smooth muscle. *J. Biol. Chem.* **274**, 3744-3752.

Galbraith, C. G. and Sheetz, M. P. (1997). A micromachined device provides a new bend on fibroblast traction forces. *Proc. Natl. Acad. Sci. USA* **94**, 9114-9118.

Goeckeler, Z. M. and Wysolmerski, R. B. (1995). Myosin light chain kinase-regulated endothelial cell contraction: the relationship between isometric tension, actin polymerization, and myosin phosphorylation. *J. Cell Biol.* **130**, 613-627.

Goeckeler, Z. M., Masaracchia, R. A., Zeng, Q., Chew, T. L., Gallagher, P. and Wysolmerski, R. B. (2000). Phosphorylation of myosin light chain kinase by p21-activated kinase PAK2. *J. Biol. Chem.* **275**, 18366-18374.

Grinnell, F. (1994). Fibroblasts, myofibroblasts, and wound contraction. *J. Cell Biol.* **124**, 401-404.

Harris, A. K., Stopak, D. and Wild, P. (1981). Fibroblast traction as a mechanism for collagen morphogenesis. *Nature* **290**, 249-251.

Hartwig, J. H., Bokoch, G. M., Carpenter, C. L., Janmey, P. A., Taylor, L. A., Toker, A. and Stossel, T. P. (1995). Thrombin receptor ligation and activated Rac uncap actin filament barbed ends through phosphoinositide synthesis in permeabilized human platelets. *Cell* **82**, 643-653.

Kimura, K., Ito, M., Amano, M., Chihara, K., Fukata, Y., Nakafuku, M., Yamamori, B., Feng, J., Nakano, T., Okawa, K. et al. (1996). Regulation of myosin phosphatase by Rho and Rho-associated kinase (Rho-kinase). *Science* **273**, 245-248.

Kureishi, Y., Kobayashi, S., Amano, M., Kimura, K., Kanaide, H., Nakano, T., Kaibuchi, K. and Ito, M. (1997). Rho-associated kinase directly induces smooth muscle contraction through myosin light chain phosphorylation. *J. Biol. Chem.* **272**, 12257-12260.

Nakanishi, S., Yamada, K., Iwahashi, K., Kuroda, K. and Kase, H. (1990). KT5926, a potent and selective inhibitor of myosin light chain kinase. *Mol. Pharmacol.* **37**, 482-488.

Pasternak, C. and Elson, E. L. (1985). Lymphocyte mechanical response triggered by cross-linking surface receptors. *J. Cell Biol.* **100**, 860-872.

Pasternak, C., Spudich, J. A. and Elson, E. L. (1989). Capping of surface receptors and concomitant cortical tension are generated by conventional myosin. *Nature* **341**, 549-551.

Petersen, N. O., McConnaughey, W. B. and Elson, E. L. (1982). Dependence of locally measured cellular deformability on position on the cell, temperature, and cytochalasin B. *Proc. Nat. Acad. Sci. USA* **79**, 5327-5331.

Pollard, T. D., Blanchoin, L. and Mullins, R. D. (2000). Molecular mechanisms controlling actin filament dynamics in nonmuscle cells. *Annu. Rev. Biophys. Biomol. Struct.* **29**, 545-576.

Raucher, D. and Sheetz, M. P. (2000). Cell spreading and lamellipodial extension rate is regulated by membrane tension. *J. Cell Biol.* **148**, 127-136.

Ren, X. D., Kiosses, W. B. and Schwartz, M. A. (1999). Regulation of the small GTP-binding protein Rho by cell adhesion and the cytoskeleton. *EMBO J.* **18**, 578-585.

Ren, X. D., Kiosses, W. B., Sieg, D. J., Otey, C. A., Schlaepfer, D. D. and Schwartz, M. A. (2000). Focal adhesion kinase suppresses Rho activity to promote focal adhesion turnover. *J. Cell Sci.* **113**, 3673-3678.

Roy, P., Petroll, W. M., Cavanagh, H. D. and Jester, J. V. (1999). Exertion of tractional force requires the coordinated up-regulation of cell contractility and adhesion. *Cell Motil. Cytoskeleton* **43**, 23-34.

Sakurada, K., Seto, M. and Sasaki, Y. (1998). Dynamics of myosin light chain phosphorylation at Ser19 and Thr18/Ser19 in smooth muscle cells in culture. *Am. J. Physiol.* **274**, C1563-1572.

Sanders, L. C., Matsumura, F., Bokoch, G. M. and de Lanerolle, P. (1999). Inhibition of myosin light chain kinase by p21-activated kinase. *Science* **283**, 2083-2085.

Sato, M., Schwarz, W. H. and Pollard, T. D. (1987). Dependence of the mechanical properties of actin/α-actinin gels on deformation rate. *Nature* **325**, 828-830.

Stopak, D. and Harris, A. K. (1982). Connective tissue morphogenesis by fibroblast traction. I. Tissue culture observations. *Dev. Biol.* **90**, 383-398.

Verkhovsky, A. B., Svitkina, T. M. and Borisy, G. G. (1999a). Network contraction model for cell translocation and retrograde flow. *Biochem. Soc. Symp.* **65**, 207-222.

Verkhovsky, A. B., Svitkina, T. M. and Borisy, G. G. (1999b). Self-polarization and directional motility of cytoplasm. *Curr. Biol.* **9**, 11-20.

Wakatsuki, T. and Elson, E. L. (2003). Reciprocal interactions between cells and extracellular matrix during remodeling of tissue constructs. *Biophys. Chem.*

Wakatsuki, T., Schwab, B., Thompson, N. C. and Elson, E. L. (2001). Effects of cytochalasin D and latrunculin B on mechanical properties of cells. *J. Cell Sci.* **114**, 1025-1036.

Worthylake, R. A. and Burridge, K. (2001). Leukocyte transendothelial migration: orchestrating the underlying molecular machinery. *Curr. Opin. Cell Biol.* **13**, 569-577.

Zahalak, G. I. (1986). A comparison of the mechanical behavior of the cat soleus muscle with a distribution-moment model. *J. Biomech. Eng.* **108**, 131-140.

Zahalak, G. I., McConnaughey, W. B. and Elson, E. L. (1990). Determination of cellular mechanical properties by cell poking, with an application to leukocytes. *J. Biomech. Eng.* **112**, 283-294.